Distinct roles of the DRY motif in rat melanin-concentrating hormone receptor 1 in signaling control

Yoshimi Aizaki[b], Kei Maruyama[b], Mitsue Nakano-Tetsuka[c], Yumiko Saito[a*]

[a]Graduate School of Integrated Arts and Sciences, Hiroshima University, Higashi-Hiroshima, 739-8521, Japan
[b]Department of Pharmacology, Saitama Medical School of Medicine, Iruma-gun, Saitama, 350-0492, Japan
[c]Department of Pharmacology, International University of Health and Welfare, Ohtawara, Tochigi, 324-8251, Japan

[*]Corresponding author: Yumiko Saito, Hiroshima University, Graduate School of Integrated Arts and Sciences, 1-7-1 Kagamiyama, Higashi-Hiroshima, 739-8521, Japan. Tel. +81-82-424-6563; fax: +81-82-442-0759.
E-mail address: yumist@hiroshima-u.ac.jp (Y. Saito)

Abbreviations: ECL, enhanced chemiluminescence; ERK1/2, extracellular signal-related kinase 1/2; FBS, fetal bovine serum; GPCR, G protein-coupled receptor; GTPγS, 5'-O-(3-thiotriphosphate); HEK293T, human embryonic kidney 293T cell; i1, intracellular loop 1; i2, intracellular loop 2; i3, intracellular loop 3; MCH, melanin-concentrating hormone; MCH1R, melanin-concentrating hormone receptor 1; TM, transmembrane.

ABSTRACT

Rhodopsin family (class A) G protein-coupled receptors possess common key residues or motifs that appear to be important for receptor function. To clarify the roles of the highly conserved amino acid triplet Asp$^{3.49}$-Arg$^{3.50}$-Tyr$^{3.51}$ (DRY motif), we examined how single-substitution mutations of the amino acids in the motif influenced specific features of rat melanin-concentrating hormone receptor 1 (MCH1R) activity. Substitution of either Asp140$^{3.49}$ or Tyr142$^{3.51}$ to Ala resulted in nonfunctional receptors, despite the retention of apparent potencies for agonist binding. These loss-of-function phenotypes may be caused by the lack of stimulation for GDP-GTP exchange observed in GTPγS-binding assays. On the other hand, substitution of Arg141$^{3.50}$ to Ala caused a 4-fold reduction in the agonist binding affinity and, concomitantly, a rightward shift of the dose-dependency curve for calcium mobilization and inhibition of cyclic AMP production. Although many experimental studies have suggested that the DRY motif is involved in maintaining the receptor in its ground state, none of the DRY motif substitutions to Ala in MCH1R led to constitutive activation, in terms of the basal signaling level for ERK1/2 activation or GTPγS binding. These data suggest that the major contribution of the DRY motif in MCH1R is to govern receptor conformation and G protein coupling/recognition.

Keywords: G protein-coupled receptor, DRY motif, Melanin-concentrating hormone, Calcium influx, Site-directed mutagenesis, Constitutive activation

1. Introduction

The Glu/Asp$^{3.49}$-Arg$^{3.50}$-Tyr$^{3.51}$ (E/DRY) sequence is located at the boundary between transmembrane (TM) domain 3 (TM3) and intracellular loop 2 (i2) of most rhodopsin family (class A) G protein-coupled receptors (GPCRs). However, other types of GPCRs, such as secretin, adhesion or glutamate GPCRs, do not possess an E/DRY sequence [14]. The high degree of conservation of this motif suggests that it must play very important roles in receptor function for rhodopsin family GPCRs but is not required for other classes of GPCRs. Many experimental and modeling studies have highlighted that both negatively and positively charged residues in the E/DRY motif are involved in regulating the receptor conformational state and/or in mediating G protein activation. In rhodopsin, Glu$^{3.49}$ and Arg$^{3.50}$ form a network of ionic interactions with Glu$^{6.30}$ in TM6, thereby constraining the receptor in an inactive conformation [20]. Indeed, a number of studies have demonstrated that mutations of Glu/Asp$^{3.49}$ in the E/DRY motif induce variable levels of constitutive activity [1,2,24,30]. Nevertheless, in different groups of receptors, mutations of Asp$^{3.49}$ did not induce constitutive activity [25]. For instance, replacement of Asp$^{3.49}$ by Ala in muscarinic m1 receptor or vasopressin V1a receptor did not affect their basal levels of activity [15,19]. On the other hand, non-conservative mutations of Arg$^{3.50}$ in many GPCRs caused impaired receptor signaling, despite unchanged binding affinities [2,10,11,23,31]. In some receptors, mutation of Arg$^{3.50}$ resulted in strongly disrupted signal transduction, with decreased agonist binding affinities [7,19]. Tyr$^{3.51}$ is the least conserved amino acid in the E/DRY motif and its roles have not been extensively studied [15,19,23].

Melanin-concentrating hormone (MCH) [17], a neuropeptide expressed in the lateral hypothalamus and zona incerta, plays important roles in complex motivated behaviors. The diverse functions of MCH are mediated by a GPCR, melanin-concentrating hormone receptor 1 (MCH1R), at least in rodents [6,26]. MCH1R belongs to the rhodopsin family of GPCRs and is phylogenetically related to receptors such as those for galanin, somatostatin and opioids [13]. Importantly, however, it is of a relatively young origin and only found in vertebrates [13]. MCH1R is widely expressed at high levels in the brain, and activates multiple signaling pathways via Gαi and Gαq coupling [6,26]. Although a second MCH receptor, MCH2R, has been identified in the human brain [16], its potential physiological functions have not yet been elucidated owing to its absence in rodents [36]. Genetic manipulations of the MCH level in mice have confirmed that MCH plays roles in feeding behavior and energy metabolism [33,34]. Furthermore, mice lacking MCH1R are lean, hyperactive, hyperphagic and hypermetabolic [20]. Rapid progress in developmental studies has revealed that selective MCH1R antagonists inhibit MCH-induced food intake in rats [4,35], and that several of these antagonists also exhibit antidepressant and anxiolytic effects [4,5]. Thus, MCH1R is an important new target for the treatment of metabolic and anxiety disorders.

Analyses of the MCH1R regulatory domains and amino acid residues participating in receptor function have been carried out. Biochemical analyses using a molecular model of MCH1R identified critical roles for Asp123 in TM3 for ligand binding [20] and Tyr255 in intracellular loop 3 (i3) for receptor trafficking to the cell surface [8]. Arg155 in i2 and a proximal dibasic motif (Arg319/Lys320) in the C-terminal tail are important for signaling [29,37], whereas the distal part of

the C-terminal tail is necessary for the internalization process [28]. However, no data have been provided regarding the functional roles of the conserved DRY motif in MCH1R. In the present study, we examined how single Ala substitutions in the DRY motif of MCH1R affected its binding, protein expression, signaling and G protein activation. Our results reveal that the DRY motif in MCH1R may play fundamental roles in governing receptor conformation and G protein coupling rather than constraining the receptor in the basal inactive conformation.

2. Materials and Methods

2.1. cDNA constructs for MCH1R

The generation of a cDNA encoding a Flag epitope tag before the first methionine in rat MCH1R was described previously [37]. Single-substitution mutations of the DRY motif, namely Flag-Asp140$^{3.49}$Ala (Flag-D140A), Flag-R141$^{3.50}$Ala (Flag-R141A) and Flag-Y142$^{3.51}$Ala (Flag-Y142A), were produced by oligonucleotide-mediated site-directed mutagenesis using a Quickchange site-directed mutagenesis kit (Stratagene, La Jolla, CA). All mutations in the MCH1R cDNA sequence were confirmed by sequencing analysis. The mutated MCH1R cDNAs were excised by digestion with EcoRI and XhoI, and inserted into the expression vector pcDNA3.1.

2.2. Cell culture and transfection

DNA was mixed with the LipofectAMINE PLUS transfection reagent (Invitrogen, Carlsbad, CA), and the mixture was diluted with OptiMEM and added to human embryonic kidney 293T (HEK293T) cells. The transfected cells were cultured in DMEM containing 10% fetal bovine serum (FBS). At 48 h after transfection, cell membranes were prepared from the cells for radioligand-binding assays and GTPγS-binding assays. For calcium influx assays, extracellular signal-related kinase 1/2 (ERK1/2) phosphorylation assays, FACScan flow cytometric analyses and immunocytochemistry, the cells were plated on 96-well plates, 12-well plates, 24-well plates and coverslips, respectively, at 24 h after transfection and cultured for a further 20-24 h. Stable transfections of HEK293T cells for expression of Flag-tagged MCH1R, D140A, R141A and Y142A were conducted according to standard procedures using zeocin selection. The levels of expression in whole cell lysates and on the cell surface were analyzed by western blotting and FACScan flow cytometry as described below.

2.3. Western blotting for MCH1R

Transiently transfected HEK293T cells were lysed in ice-cold buffer (50 mM Tris-HCl pH 8.0, 150 mM NaCl, 1% Triton X-100, 0.1% SDS, 0.5% deoxycholate and a protease inhibitor mixture (Roche, Indianapolis, IN)) at 4°C, and then cleared by centrifugation at 18,500 × *g* for 20 min at 4°C. The protein concentration of each supernatant was determined using a BCA protein assay kit (Pierce, Rockford, IL). Aliquots containing 15 μg of total protein were separated by SDS-PAGE and electrotransferred to Hybond-P PVDF membranes (GE Healthcare UK Ltd., Little Chalfont, UK). After blocking with 5% skim milk, Flag-MCH1R on the membrane was detected using an anti-Flag M2 antibody, followed by a horseradish peroxidase-conjugated goat anti-mouse IgG antibody. The

reactive bands were visualized with enhanced chemiluminescence (ECL) substrates (GE Healthcare UK Ltd.) and analyzed using Scion Image (Scion Corporation, Frederick, MD).

2.4. FACScan flow cytometric analysis of cell surface receptors

Transiently transfected HEK293T cells were fixed and then incubated with an anti-Flag M2 antibody in PBS containing goat serum for 1 h. Next, the cells were washed with PBS and incubated with a FITC-conjugated goat anti-mouse IgG secondary antibody for 1 h. The cells were collected and analyzed using a FACScan flow cytometer (Becton Dickinson Immunocytometer Systems Inc., Franklin Lakes, NJ). Cells were gated by light scatter or exclusion of propidium iodide, and 10,000 cells were acquired for each time point. The mean fluorescence of all the cells minus the mean cell fluorescence with the FITC-conjugated secondary antibody alone was used for the calculations.

2.5. Radioligand-binding assay

Membrane preparations derived from transfected HEK293T cells were subjected to radioligand-binding assays according to a previously described procedure [34]. The membrane fractions (15 μg of protein/assay) were incubated with increasing concentrations (0.01-6 nM) of [^{125}I](Phe^{13}, Tyr^{19})MCH (GE Healthcare UK Ltd.) in the presence or absence of 1 μM non-labeled MCH (Peptide Institute, Osaka, Japan) in assay buffer (50 mM Tris-HCl pH 7.4, 1 μM phosphoramidon, 0.5 mM PMSF and 0.2% BSA) at room temperature for 2 h. The binding reactions were terminated by rapid filtration through GF/C glass filter plates presoaked in 0.2% polyethylenimine, followed by three washes with PBS. The radioactivity retained on each filter was determined using a γ-counter. Specific binding was defined as the difference between the total binding and the non-specific binding.

2.6. Confocal immunofluorescence microscopy

Transiently transfected HEK293T cells were fixed, transferred with or without permeabilization (0.05% Triton X-100 in PBS) into a blocking solution for 30 min, and then incubated with an anti-Flag M2 antibody for 1 h. The anti-Flag M2 antibody was detected using an Alexa Fluor 488-conjugated goat anti-mouse IgG secondary antibody (Molecular Probes, Eugene, OR). Fluorescence imaging was performed using a TE300/Radiance2000 confocal microscope (Bio-Rad Laboratories, Hercules, CA).

2.7. Measurement of intracellular Ca^{2+}

Transiently transfected cells seeded on 96-well plates (Becton Dickinson) were loaded with a non-wash calcium dye (Calcium Assay Kit; Molecular Devices, Sunnyvale, CA) in Hank's balanced salt solution containing HEPES (pH 7.5) for 1 h at 37°C. For each concentration of MCH, the level of $[Ca^{2+}]_i$ was detected using a Flexstation imaging plate reader (Molecular Devices) [27]. Data were expressed as the fluorescence (arbitrary units) versus time. The EC_{50} values for MCH were obtained from sigmoidal fits using a nonlinear curve-fitting program (Prism version 3.0; GraphPad Software, San Diego, CA).

2.8. ERK1/2 phosphorylation and immunoblotting

Transiently transfected cells were serum-starved and then stimulated with 5 μM MCH in Hank's balanced salt solution containing 20 mM HEPES (pH 7.5) for 5 min at 37°C. After aspiration of the media, the cells were lysed in lysis buffer (50 mM Tris-HCl pH 7.5, 150 mM NaCl, 5 mM EDTA, 20 mM NaF, 1% NP-40, 0.1% SDS, 0.5% deoxycholate, 5 μg/ml leupeptin and 1 mM PMSF) and centrifuged at 10,000 × *g* at 4°C for 30 min. Aliquots containing 15 μg of total protein were resolved by SDS-PAGE and transferred to PVDF membranes for detection of phosphorylated ERK1/2. The membranes were probed with an anti-phospho-ERK1/2 monoclonal antibody (Santa Cruz Biotechnology, Santa Cruz, CA), and the phosphorylated protein levels were detected by ECL.

2.9. Measurement of cAMP production

For measurement of forskolin-induced cAMP accumulation, only stably transfected cells could be used because we were unable to obtain reproducible data with transiently transfected cells. This may be due to forskolin-induced accumulation of non-transfected cells among the transiently transfected cells causing a high background for the inhibition assay. The cells were preincubated with a cAMP assay buffer (Hank's balanced salt solution supplemented with 20 mM HEPES and 0.3 mM 3-isobutyl-1-methylxanthine, pH 7.5) for 10 min, and then incubated with 1 μM forskolin and various concentrations of MCH for 15 min. The reactions were terminated with 0.3 N HCl, and the levels of extracted intracellular cAMP were measured using a radioimmunoassay kit (Yamasa, Kyoto, Japan) according to the manufacturer's protocol.

2.10. GTPγS-binding assay

Aliquots of the membrane proteins isolated for the radioligand-binding assays were incubated in GTPγS binding buffer (20 mM HEPES-NaOH pH 7.5, 100 mM NaCl, 5 mM $MgCl_2$, 0.2% BSA and 3 μM GDP) containing 0.2 nM [^{35}S]GTPγS and various concentrations of MCH for 30 min at 30°C [37]. To determine the non-specific binding, unlabeled GTPγS was added to the binding mixtures to a final concentration of 100 μM. The bound [^{35}S]GTPγS was separated from free [^{35}S]GTPγS by rapid filtration through GF/C filters and washed with ice-cold binding buffer. The radioactivities of the filters were counted in the scintillation cocktail Emulsion-Scintillator Plus (Packard Bioscience, Groningen, Netherlands) using a liquid scintillation counter.

3. Results

3.1. Protein expression in cells expressing Flag-tagged MCH1R and DRY mutants

First, we transiently transfected Flag-tagged MCH1R or DRY mutants into HEK293T cells and examined the receptor expression levels by western blotting analysis with the anti-Flag M2 antibody. Several immunoreactive bands were detected in the SDS/detergent-soluble supernatant isolated from cells expressing Flag-MCH1R (Fig. 1A). Some bands matched the predicted molecular masses of approximately 38, 44, 45 and 60 kDa [37], although additional immunoreactive bands were observed at 45-60 kDa. Our previous study revealed that the 38-kDa band was the non-glycosylated form of MCH1R [27], while the three higher molecular mass bands were different N-linked glycosylated forms. The higher molecular mass immunoreactive bands were also detected for Flag-R141A, although the intensities were moderately reduced. The migration patterns of Flag-D140A and Flag-Y142A were very similar and drastic reductions in the intensities of the higher molecular mass bands were observed compared with those of Flag-MCH1R. As determined by imaging analysis, the 60-kDa band intensities were decreased by 81% and 73% for Flag-D140A and Flag-Y142A, respectively, but only 31% for Flag-R141A. The decreased intensities of the 60-kDa band seemed to be caused by a lack of appropriate glycosylation of the mutant receptors, as previously described in an N-linked glycosylation study and other studies of MCH1R [27,37].

3.2. Cell surface expression and ligand-binding properties of Flag-tagged MCH1R and DRY mutants

The cell surface expression levels of Flag-tagged MCH1R and DRY mutants were evaluated by FACScan flow cytometry using the anti-Flag M2 antibody (Fig. 1B). Transient transfection of Flag-D140A and Flag-Y142A yielded 43% and 42% of the Flag-MCH1R level, respectively, whereas Flag-R141A yielded 78% of the Flag-MCH1R level. Consistent with the FACScan data, saturation binding of [^{125}I](Phe^{13}, Tyr^{19})MCH to cell membranes isolated from cells transiently transfected with each of the mutant receptors revealed lower levels of cell surface expression compared with Flag-MCH1R (Table 1). Furthermore, the affinity constants of Flag-D140A and Flag-Y142A for agonists showed slight, but significant, decreases relative to that of Flag-MCH1R, while that of Flag-R141A exhibited an almost 4-fold decrease.

3.3. Immunocytochemical localizations of Flag-tagged MCH1R and DRY mutants

We investigated the subcellular localizations of Flag-tagged MCH1R and DRY mutants using immunological detection techniques. In non-permeabilized cells, Flag-D140A and Flag-Y142A were clearly localized in the plasma membrane, although their labeling intensities were decreased compared with those of Flag-MCH1R and Flag-R141A (Fig. 2, left). In permeabilized cells, Flag-MCH1R was predominantly detected in the plasma membrane, while Flag-D140A and Flag-Y142A were both detected intracellularly (Fig. 2, right). Flag-R141A was detected in the cytoplasm as well as in the plasma membrane. These subcellular localizations of the mutants were consistent with the data obtained in the FACScan analysis. These results suggest that the D140A and Y142A mutations produce similar phenotypes in terms of the levels of protein expression and cell surface expression, subcellular localizations and kinetics of radioligand binding.

3.4. MCH-induced signaling in cells expressing Flag-tagged MCH1R and DRY mutants

Next, the capabilities of the mutant receptors for inducing intracellular signals in response to MCH were examined. First, MCH-induced calcium influxes were assayed in transiently transfected cells using a Flexstation imaging plate reader (Fig. 3A). The dose-response curve for Flag-R141A was shifted to the right, and showed a 36-fold higher EC50 value for MCH with a nearly 20% reduction in the maximal response (Table 2). In marked contrast, both Flag-D140A and Flag-Y142A showed complete loss of the MCH-stimulated calcium influx, even when challenged with high concentrations up to 10 μM.

MCH can effectively activate ERK1/2 phosphorylation [14]. Consistent with these previous data, we observed that addition of MCH to HEK293T cells expressing Flag-MCH1R after transient transfection led to dose-dependent activation of ERK1/2 phosphorylation. The response was maximal after 5 min of stimulation with 1 μM MCH, and returned to the non-stimulated level after 10 min. The temporal pattern of ERK1/2 activation for Flag-R141A was very similar to that for Flag-MCH1R (data not shown). The responses of ERK1/2 phosphorylation stimulated by 1 μM MCH were 225% for Flag-MCH1R and 163% for Flag-R141A relative to the non-stimulated level, while no activation was observed for Flag-D140A and Flag-Y142A (Fig. 3B, Table 2), even after increasing the dose of MCH to 10 μM or changing the time of the MCH stimulation. It is also noteworthy that the basal level of ERK1/2 phosphorylation was not enhanced by any of the mutants (Fig. 3B), indicating that none of the mutants showed an enhanced level of constitutive activity.

MCH stimulates a calcium influx and activates ERK1/2 phosphorylation via Gαq- and Gαi/o-mediated pathways, while Gαi/o activation via MCH1R results in a decrease in adenylyl cyclase and reduced cAMP production [6,14,26]. Next, we examined these abilities in the mutants by measuring forskolin-induced cAMP accumulation using stably transfected cells (Fig. 3C, Table 2). Flag-R141A showed an 80-fold higher EC50 value with a nearly 30% reduction in the maximum inhibition, while Flag-MCH1R showed a 60% reduction. Thus, the R141A mutation affects both Gαq- and Gαi/o-mediated signaling and produces impaired responses in multiple signaling pathways. In addition, no significant difference in the basal levels of cAMP accumulation was detected between Flag-MCH1R and Flag-R141A (data not shown). Although stable cell clones for Flag-D140A and Flag-Y142A were established, none of the clones were suitable for use in forskolin-induced cAMP accumulation assays because restricted amounts of the mutant receptor proteins were expressed on the cell surface, as determined by FACScan analysis. Indeed, the levels of cell surface expression of Flag-D140A and Flag-Y142A were only about 10% of the level of Flag-MCH1R. This may be due to continuous improper glycosylation and/or failure of efficient trafficking of Flag-D140A and Flag-Y142A to the plasma membrane under long-term culture for antibiotic selection.

To better characterize the properties of the mutant receptors, both the basal and MCH-stimulated [^{35}S]GTPγS binding were examined in the membranes of cells transiently transfected with Flag-tagged MCH1R and mutant receptors (Fig. 4). Consistent with our previous report, Flag-MCH1R revealed dose-dependent binding of GTPγS with an EC50 value of 15.7 ± 1.6 nM, while the value for Flag-R141A was 77.2 ± 3.9 nM. The maximal amount of binding for

Flag-MCH1R with 0.3 μM MCH was 155.8%, while that for Flag-R141A with 3 μM MCH was 126.5%. In contrast, Flag-D140A and Flag-Y142A showed no GTPγS binding, even with 10 μM MCH. Therefore, Flag-D140A and Flag-Y142A appeared to show loss-of-function phenotypes for signaling (Table 2), which may be caused by the lack of stimulation for GDP-GTP exchange detected in the GTPγS-binding assays. Regarding the basal GTPγS binding, the values were 105.5 ± 4.7%, 102.9 ± 3.8% and 94.2 ± 3.0% for Flag-D140A, Flag-R141A and Flag-Y142A, respectively (n=3, mean ± SEM), relative to Flag-MCH1R as 100%. Thus, none of the mutant receptors exhibited significantly higher basal GTPγS binding than Flag-MCH1R, once again indicating a lack of involvement of the DRY motif in constitutive activation.

4. Discussion

In the present study, Ala substitutions in MCH1R were used to examine the effects of a highly conserved DRY motif on the receptor expression, localization, binding, signaling and G protein coupling in HEK293T cells. Structure-function relationship studies have traditionally and mainly been performed on monoamine-binding GPCRs [2,24,30], and the conclusion that the E/DRY motif constrains the receptor in an inactive state has been used to generalize its role for the entire rhodopsin family of GPCRs. However, we found that single-substitution mutations of the amino acids in the DRY motif of MCH1R with Ala showed no indications of constitutive activity. Thus, the widely accepted model may not apply to MCH1R with DRY motif mutations, and MCH1R may belong to another group of GPCRs that are resistant to DRY-mediated constitutive activity. Rovati et al. [25] discriminated at least two phenotypes for the E/DRY motif in rhodopsin family GPCRs. In the CAM group of receptors, the E/DRY motif plays distinct roles in the equilibrium between active and inactive conformations of GPCRs, and is involved in constraining GPCRs in their inactive ground state. In the CIM group of receptors, the motif is involved in mediating G protein coupling/recognition, because E/D$^{3.49}$ mutations do not induce constitutive activity. Thus, MCH1R can be classified as a CIM-type receptor.

We found that Ala substitution of Asp140$^{3.49}$ in MCH1R completely disrupted the signaling properties in transiently transfected cells. The loss of function following Asp$^{3.49}$ substitution to Ala seems to be in agreement with previous observations in cells transiently transfected with M1 muscarinic receptor or vasopressin V1a receptor mutants [15,19]. These two mutants abolished agonist binding owing to severe reductions in receptor expression (10% of the wild-type) at the cell surface. However, our data for MCH1R are different from this phenotype. The D140A mutant of MCH1R still maintained a cell surface expression level of 40% relative to the wild-type level with apparent affinities for agonist binding. Ala substitution of Tyr142$^{3.51}$ in MCH1R also resulted in loss of MCH-mediated signaling with retained agonist binding affinity. To the best of our knowledge, the loss-of-function phenotypes with agonist binding observed for the present D140A and Y142A mutants have not been found following mutations of Asp$^{3.49}$ and Tyr$^{3.51}$ in other GPCRs. On the other hand, substitution of Arg$^{3.50}$ in MCH1R to Ala resulted in a 4-fold decrease in the binding affinity and showed a right shift of the dose-dependency curve for calcium mobilization and inhibition of cAMP accumulation. These features suggest that Arg141$^{3.50}$ may be in a position that can modulate the

agonist-binding pocket, and conceivably, decrease accessibility for G protein coupling. Therefore, similar to the results obtained for other GPCRs, our data support that $Arg^{3.50}$ in MCH1R is one of the major determinants for governing receptor conformation and G protein activation [1,2,7,10,11,15,23,25]. A crucial role for $Arg^{3.50}$ in the active state of GPCRs has also been indicated in a very recent report [32]. In that report, Scheerer et al. determined the activated structure of opsin in a complex with the receptor-binding peptide fragment of the Gα protein (the C-terminus of the Gα subunit: GαCT), and revealed how the side chains of the E/DRY motif are involved in Gα protein binding. In their model, Arg135 ($Arg^{3.50}$) of the DRY motif is allowed to swing into the center of the GαCT binding and becomes stabilized by Tyr223. Subsequently, it interacts with the main-chain carbonyl of GαCT residue Cys347. Thus, $Arg^{3.50}$ in the E/DRY motif seems to have a dual role in both the inactive and active conformations of GPCRs.

As described above, the D140A and Y142A mutations caused reductions in the cell surface expression levels in transiently transfected HEK293T cells compared with that of MCH1R. The decreased cell surface expression levels of the D140A and Y142A mutants could not be explained by receptor downregulation as a consequence of receptor internalization [15,19] because promotion of MCH-induced internalization of these two mutants compared with the wild-type receptor was not observed by microscopy (data not shown). Our western blotting analysis revealed 70-80% reductions in the band intensities of the 60-kDa receptor for the D140A and Y142A mutants, suggesting immature forms of the receptor with much lower extents of glycosylation. Very similar correlations between the glycosylation levels of the 60-kDa receptor and the cell surface expression levels of MCH1R were observed in triple-substituted mutants in intracellular loop 1 (i1; K67Q/K68Q/K70Q) and i3 (K153Q/R155Q/K156Q), respectively [37]. Together with interpretation of a previous N-linked glycosylation study of MCH1R [27], the reductions in cell surface expression observed for the D140A and Y142A mutants appear to be clearly related to lower extents of glycosylation, which lead to incorrect intracellular trafficking of the receptor. However, the loss-of function phenotypes of the D140A and Y142A mutants were not due to the loss of carbohydrate moieties because MCH1R still displays functional signaling after disruption of all its glycosylation sites accompanied by a 60% reduction in cell surface expression [27]. The extreme insensitivities of the D140A and Y142A mutants for signaling may be caused by unusually misfolded receptor architectures and/or receptor instabilities, in which G protein coupling or recognition is severely disrupted.

By phylogenetic analysis, the rhodopsin family forms four main groups with 13 sub-branches [12]. The monoamine-binding GPCRs and rhodopsin receptors, in which mutations of the E/DRY motif lead to constitutive activity, belong to the α-group [1,2,24,30]. On the other hand, MCH1R belongs to the entirely different γ-group, which contains three main branches (MCH receptor cluster, SOG receptor cluster and chemokine receptor cluster). Further analysis of entire Genscan data sets from sequenced genomes in 13 species revealed that the MCH receptor branch is one of the youngest in the γ-group, since this cluster is found in vertebrates but not in more distant species, such as *Ciona*, insects or nematodes [13]. Therefore, in light of the phylogenetic perspective, it is of significant interest to carry out structural comparisons of the signaling motifs with rhodopsin family GPCRs, and find a common pattern among individual groups and sub-branches. To the best of our knowledge,

approximately 24 GPCRs have functional pharmacological data regarding the E/DRY motif to date [23, 25]. This number may not sufficient at the present time to predict the likely phenotype for a receptor (not mutated in the motif) by the phylogenetic pattern. For example, the γ-group includes 59 GPCRs, but pharmacological data in the E/DRY motif are only available for two receptors, namely MCH1R (no constitutive activity) and μ-opioid receptor (constitutive activity) [18]. Thus, it is necessary to perform more systematic functional experiments incorporating a broader phylogenetic overview, and these studies should provide a novel consensus picture for the role of the highly conserved E/DRY motif.

In summary, we have provided evidence that MCH1R belongs to a distinct group of rhodopsin family GPCRs that may utilize the residues in the DRY motif to govern receptor conformation and G protein coupling. Further studies are required to clarify the responsible amino acid residues or domains that lead to constitutive activation or a more active hypersensitive form of MCH1R. These findings will contribute to approaches for building a functional 3-dimensional model of MCH1R, and should be the proving grounds for therapeutic applications toward obesity and some mental diseases.

Acknowledgments

We thank Dr. Akira Hikosaka (Graduate School of Integrated Arts and Sciences, Hiroshima University) for helpful advice regarding the phylogenetic relationships in GPCRs. This study was supported by grants from the Skylark Food Science Foundation (to Y.S.), the Life-Science Foundation (to Y.S.) and the KAKENHI (No.155000266 to Y.S.).

REFERENCES

[1] Acharya S, Karnik SS. Modulation of GDP release from transducin by the conserved Glu134-Arg135 sequence in rhodopsin. J Biol Chem 1996; 271: 25406-25411.

[2] Alewijnse AE, Timmerman H, Jacobs EH, Smit MJ, Roovers E, Cotecchia S, Leurs R. The effect of mutations in the DRY motif on the constitutive activity and structural instability of the histamine H_2 receptor. Mol Pharmacol 2000; 57: 890-898.

[3] Arora KK, Zhengyi Z, Cheng Z, K.J. Catt KJ. Mutations of the conserved DRS motif in the second intracellular loop of the gonadotropin-releasing hormone receptor affect expression, activation, and internalization. Mol Endocrinol 1997; 11: 1203-1212.

[4] Borowsky B, Durkin MM, Ogozalek K, Marzabadi MR, DeLeon J, Lagu B, Heurich R, Lichtblau H, Shaposhnik Z, Daniewska I, Blackburn TP, Branchek TA, Gerald C, Vaysse PJ, Forray C. Antidepressant, anxiolytic and anorectic effects of a melanin-concentrating hormone-1 receptor antagonist. Nat Med 8; 2002: 825-830.

[5] Chaki S, Funakoshi T, Hirota-Okuno S, Nishiguchi M, Shimazaki T, Iijima M, Grottick AJ, Kanuma K, Omodera K, Sekiguchi Y, Okuyama S, Tran TA, Semple G, Thomsen W. Anxiolytic- and antidepressant-like profile of ATC0065 and ATC0175: nonpeptidic and orally active melanin-concentrating hormone receptor 1 antagonists. J Pharmacol Exp Ther 2005; 313: 831-839.

[6] Chambers J, Ames RS, Bergsma D, Muir A, Fitgerals LR, Hervieu G, Dytko GM, Foley JJ, Martin J, Liu WS, Park J, Ellis C, Ganguly S, Konchar S, Cluderray J, Leslie R, Wilson S, Sarau HM. Melanin-concentrating hormone is the cognate ligand for the orphan G-protein-coupled receptor SLC-1. Nature 1999; 400: 261-265.

[7] Chung DA, Wade SM, Fowler CB, Woods DD, Abada PB, Mosberg HI, Neubig RR. Mutagenesis and peptide analysis of the DRY motif in the alpha2A adrenergic receptor: evidence for alternate mechanisms in G protein-coupled receptors. Biochem Biophys Res Commun. 2002; 293: 1233-1241.

[8] Fan J, Perry SJ, Gao Y, Schwarz DA, Maki RA. A point mutation in the human melanin concentrating hormone receptor 1 reveals an important domain for cellular trafficking. Mol Endocrinol 2005; 2579-2590.

[9] Fanelli F, Barbier P, Zanchentta D, De Benedetti PG, Chini B. Activation mechanism of human oxytocin receptor: a combined study of experimental and computer-simulated mutagenesis. Mol Pharmacol 1999; 56: 214-225.

[10] Feng W, Song ZH. Effects of D3.49A, R3.50A and A6.34E mutations on ligand binding of the activation of the cannabinoid-2(CB2) receptor. Biochem Pharmacol 2003; 65: 1077-1085.

[11] Franke RR, Sakmar TP, Graham RM, Khorana HG. Structure and function in rhodopsin. Studies of the interaction between the rhodopsin cytoplasmic domain and transducin. J Biol Chem 1992; 267: 14767-14774.

[12] Fredriksson R, Lagerstrom MC, Lundin L-G, Schioth HB. The G-protein-coupled receptors in the human genome form five families. Phylogenetic analysis, paralogon groups, and fingerprints. Mol Pharmacol. 2003; 63: 1256-1272.

[13] Fredriksson R, Schioth HB. The repertoire of G-protein-coupled receptors in fully sequenced genomes. Mol Pharmacol 2005; 67: 1414-1425.

[14] Hawes BE, Kil E, Green B, O'Neill K, Fried S, Graziano MP. The melanin-concentrating hormone couples to multiple G proteins to activate diverse intracellular signaling pathways. Endocrinology 2000; 141: 4524-4532.

[15] Hawtin SR. Charged residues of the conserved DRY triplet of the vasopressin V1a receptor provide molecular determinants for cell surface delivery and internalization. Mol Pharamacol 2005; 68: 1172-1182.

[16] Hill J, Duckworth M, Murdock P, Rennie G, Sabido-David C, Ames RS, Szekeres P, Wilson S, Bergsma DJ, Gloger IS, Levy DS, Chambers JK, Muir AI. Molecular cloning and functional characterization of MCH2, a novel human MCH receptor. J Biol Chem 2001; 276: 20125-20129.

[17] Kawauchi H, Kawazoe I, Tsubokawa M, Kishida M, Baker BL. Characterization of melanin-concentrating hormone in chum salmon pituitaries. Nature 1983; 305: 321-323.

[18] Li J, Huang P, Chen C, de Riel JK, Weinstein H, Liu-Chen LY. Constitutive activation of the mu opioid receptor by mutation of D3.49(164), but not D3.32(147): D3.49(164) is critical for stabilization of the inactive form of the receptor and for its expression. Biochemistry 2001; 40:12039-12050.

[19] Lu ZL, Curtis CA, Jones PG, Pavia J, Hulme EC, The role of the aspartate-arginine-tyrosine triad in the m1 muscarinic receptor: mutations of aspartate 122 and tyrosine 124 decrease receptor expression but do not abolish signaling. Mol Pharmacol 1997; 51: 234-241.

[20] MacDonald D, Murgolo N, Zhang R, Durkin JP, Yao X, Strader CD, Graziano MP. Molecular characterization of the melanin-concentrating hormone/receptor complex: Identification of critical residues involved in binding and activation. Mol Pharmacol 2000; 58: 217-225.

[21] Marsh DJ, Weingarth DT, Novi DE, Chen HY, Trumbauer ME, Chen AS, Guan XM, Jiang MM, Feng Y, Camacho RE, Shen Z, Frazier EG, Yu H, Metzger JM, Kuca SJ, Shearman LM, Gopal-Truter S, MacNeil DJ, Strack AM, MacIntyre DE, Van der Ploeg LH, Qian S. Melanin-concentrating hormone 1 receptor-deficient mice are lean, hyperactive, and hyperphagic and have altered metabolism. Proc Natl Acad Sci USA 2002; 99: 3240-3245.

[22] Palczewski K, Takashi Kumasaka T, Hori T, Behnke CA, Motoshima H, Fox BA, Trong IL, Teller DC, Okada T, Stenkamp RE, Yamamoto M, Masashi Miyano M. Crystal structure of rhodopsin: A G protein-coupled receptor. Science 2000; 289: 739-745.

[23] Proulx CD, Holleran BJ, Boucard AA, Escher E, Guillemette G, Leduc R. Mutational analysis of the conserved $Asp^{2.50}$ and ERY motif reveals signaling bias of the urotensin II receptor. Mol Pharmacol 2008, 74: 552-561.

[24] Rasmussen SG, Jensen AD, Liapakis G, Ghanouni P, Javitch JA, Gether U. Mutation of a highly conserved aspartic acid in the beta2 adrenergic receptor: constitutive activation, structural instability, and conformational rearrangement of transmembrane segment 6. Mol Pharmacol 1999; 56: 175-184.

[25] Rovati EG, Capra V, Neubig RR. The highly conserved DRY motif of class A G-protein-coupled receptors: beyond the ground state. Mol Pharmacol 2007; 71: 959-964.

[26] Saito Y, Nothacker HP, Wang Z, Lin SHS, Leslie F, Civelli O. Molecular characterization of the melanin-concentrating-hormone receptor. Nature 1999; 400: 265-269.

[27] Saito Y, Tetsuka M, Kawamura Y, Li Y, Maruyama K. Role of asparagine-linked oligosaccharides in the function of the melanin-concentrating hormone (MCH) receptor 1. FEBS Lett 2003; 533: 229-234.

[28] Saito Y, Tetsuka M, Li Y, Kurose H, Maruyama K. Properties of rat melanin-concentrating hormone receptor 1 internalization. Peptide 2004; 25: 1597-1604.

[29] Saito Y, Tetsuka M, Saito S, Imai K, Yoshikawa A, Doi H, Maruyama K. Arginine residue 155 in the second intracellular loop plays a critical role in rat melanin-concentrating hormone receptor 1. Endocrinology 2005; 146: 3452-3462.

[30] Scheer A, Fanelli F, Costa T, De Benedetti PG, Cotecchia S. The activation process of the α1B-adrenergic receptor: potential role of protonation and hydrophobicity of a highly conserved aspartate. Proc Natl Acad Sci USA 1997; 94: 808-813.

[31] Scheer A, Costa T, Fanelli F, De Benedetti PG, Mhaouty-Kodja S, Abuin L, Nenniger-Tosato M, Cotecchia S, Mutational analysis of the highly conserved arginine within the Glu/Asp-Arg-Tyr motif of the alpha(1b)-adrenergic receptor: effects on receptor isomerization and activation. Mol Pharmacol 2000; 57: 219-231.

[32] Scheerer P, Park JH, Hildebrand PW, Kim YJ, Krau N, Choe H-W, Klaus Peter Hofmann KP, Ernst OP. Crystal structure of opsin in its G-protein-interacting conformation: Nature 2008; 455:497-502.

[33] Segal-Lieberman G, Bradley RL, Kokkotou E, Carlson M, Trombly DJ, Wang X, Bates S, Myers MG, Flier Jr JS, Maratos-Flier E. Melanin-concentrating hormone is a critical mediator of the leptin-deficient phenotype. Proc Natl Acad Sci USA 2003; 100: 10085-10090.

[34] Shimada M, Tritos NA, Lowell BB, Flier JS, Maratos-Flier E. Mice lacking melanin-concentrating hormone are hypophagic and lean. Nature 1998; 396: 670-674.

[35] Takekawa S, Asami A, Ishihara Y, Terauchi J, Kato K, Shimomura Y, Mori M, Murakoshi H, Kato K, Suzuki N, Nishimura O, Fujino M. T-226296: A novel, orally active and selective melanin-concentrating hormone receptor antagonist. Eur J Pharmacol 2002; 438: 129-135.

[36] Tan CP, Sano H, Iwaasa H, Pan J, Sailer AW, Hreniuk DL, Feighner SD, Palyha OC, Pong SS, Figueroa DJ, Austin CP, Jiang MM, Yu H, Ito J, Ito M, Guan XM, MacNeil DJ, Kanatani A, Van der Ploeg LH, Howard AD. Melanin-concentrating hormone receptor subtypes 1 and 2: Species-specific gene expression. Genomics 2002; 79: 785-792.

[37] Tetsuka M, Saito Y, Imai K, Doi H, Maruyama K. The basic residues in the membrane-proximal C-terminal tail of the rat melanin-concentrating hormone receptor 1 are required for receptor function. Endocrinology 2004; 145: 3712-3723.

Figure Legends

Figure 1. Protein expression levels in cells transiently transfected with cDNAs for Flag-tagged wild-type and mutant MCH1Rs. (A) Protein expression levels in transiently transfected HEK293T cells evaluated by western blotting. Following cell lysis with ice-cold SDS/detergent solution, aliquots containing 15 μg of total protein were separated by SDS-PAGE, transferred to a PVDF membrane and immunoblotted with an anti-Flag M2 antibody. (B) Cell surface expression levels evaluated by FACScan flow cytometric analysis. The percentage with respect to Flag-MCH1R (100%) was calculated for each mutant. The data represent the means ± SEM of at least three independent experiments performed in duplicate.

Figure 2. Immunolocalization of Flag-tagged MCH1R and mutant receptors with an anti-Flag M2 antibody. The cellular localizations were compared using transiently transfected non-permeabilized (-TX: without Triton X-100) and permeabilized (+TX: with Triton X-100) cells. Vector-transfected cells incubated with the anti-Flag M2 antibody showed no significant staining (data not shown). Bar = 10 μm.

Figure 3. MCH-induced signaling and G protein coupling in transfected cells. (A) Dose-response relationships of MCH-mediated calcium influxes in viable HEK293T cells expressing Flag-tagged MCH1R and mutant receptors. Fluorescence units are shown for Flag-tagged MCH1R and Flag-D140A, Flag-R141A and Flag-Y142A mutants. Data represents the means ± SEM of duplicate determinations, and two additional experiments gave similar results. (B) ERK1/2 phosphorylation in transfected HEK293T cells expressing Flag-tagged MCH1R and mutant receptors. Transfected cells were serum-starved and then stimulated with 1 μM MCH for 5 min at 37°C. Cell lysates were analyzed by immunoblotting with an anti-phospho-ERK1/2 antibody (upper) after separation by SDS-PAGE and transfer to a PVDF membrane. The membrane was subsequently stripped and reprobed with an anti-ERK1/2 antibody to control for equal loading (lower). Representative results are shown. (C) Forskolin-stimulated cAMP inhibition assays. Inhibition of forskolin-induced cAMP accumulation in HEK293T cells stably transfected with Flag-tagged MCH1R and Flga-R141A mutant is shown. Data were normalized to the amounts of cAMP in 1 μM forskolin-stimulated cells (set at 100%). All experiments were independently performed three times in duplicate, and representative results are shown.

Figure 4. MCH-stimulated [^{35}S]GTPγS binding to Flag-tagged MCH1R and mutant receptors. HEK293T cells were transfected with Flag-tagged MCH1R and Flag-D140A, Flag-R141A and Flag-Y142A mutants. After 2 days, the cells were collected and the membrane fractions were isolated. The membrane proteins (5 μg) were incubated with 0.2 nM [^{35}S]GTPγS and various concentrations of MCH (1 nM-30 μM) in GTPγS binding buffer for 30 min at 30°C. The amounts of radioactivity bound to the membrane proteins are shown for Flag-tagged MCH1R, Flag-D140A, Flag-R141A and Flag-Y142A mutants. All experiments were independently performed three times in triplicate, and representative results are shown as the means ± SEM.

Fig.1

A

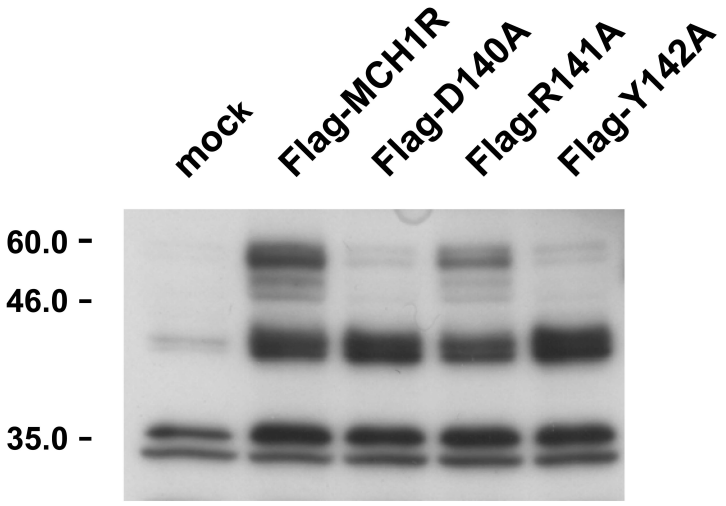
mock
Flag-MCH1R
Flag-D140A
Flag-R141A
Flag-Y142A
60.0
46.0
35.0

B

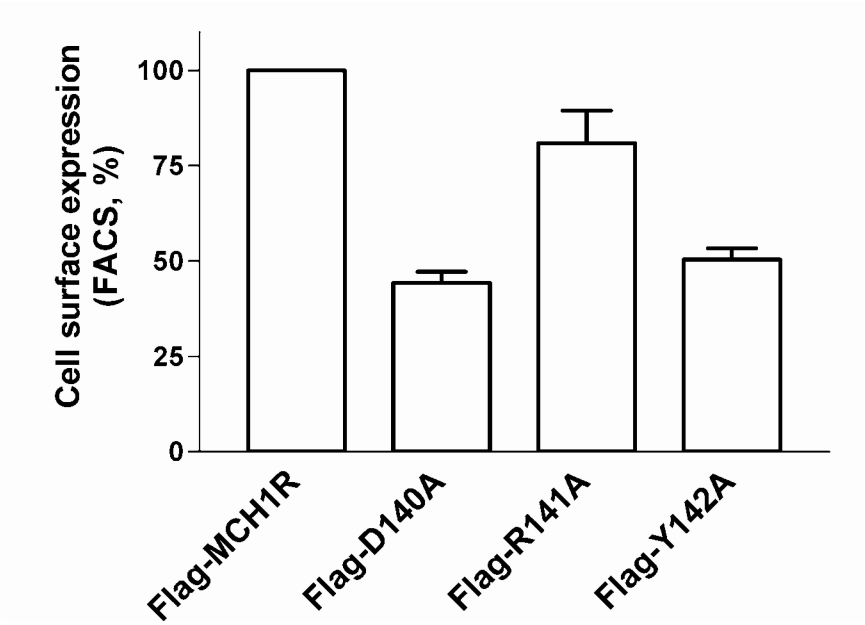
Cell surface expression
(FACS, %)
100
75
50
25
0
Flag-MCH1R
Flag-D140A
Flag-R141A
Flag-Y142A

Fig.2

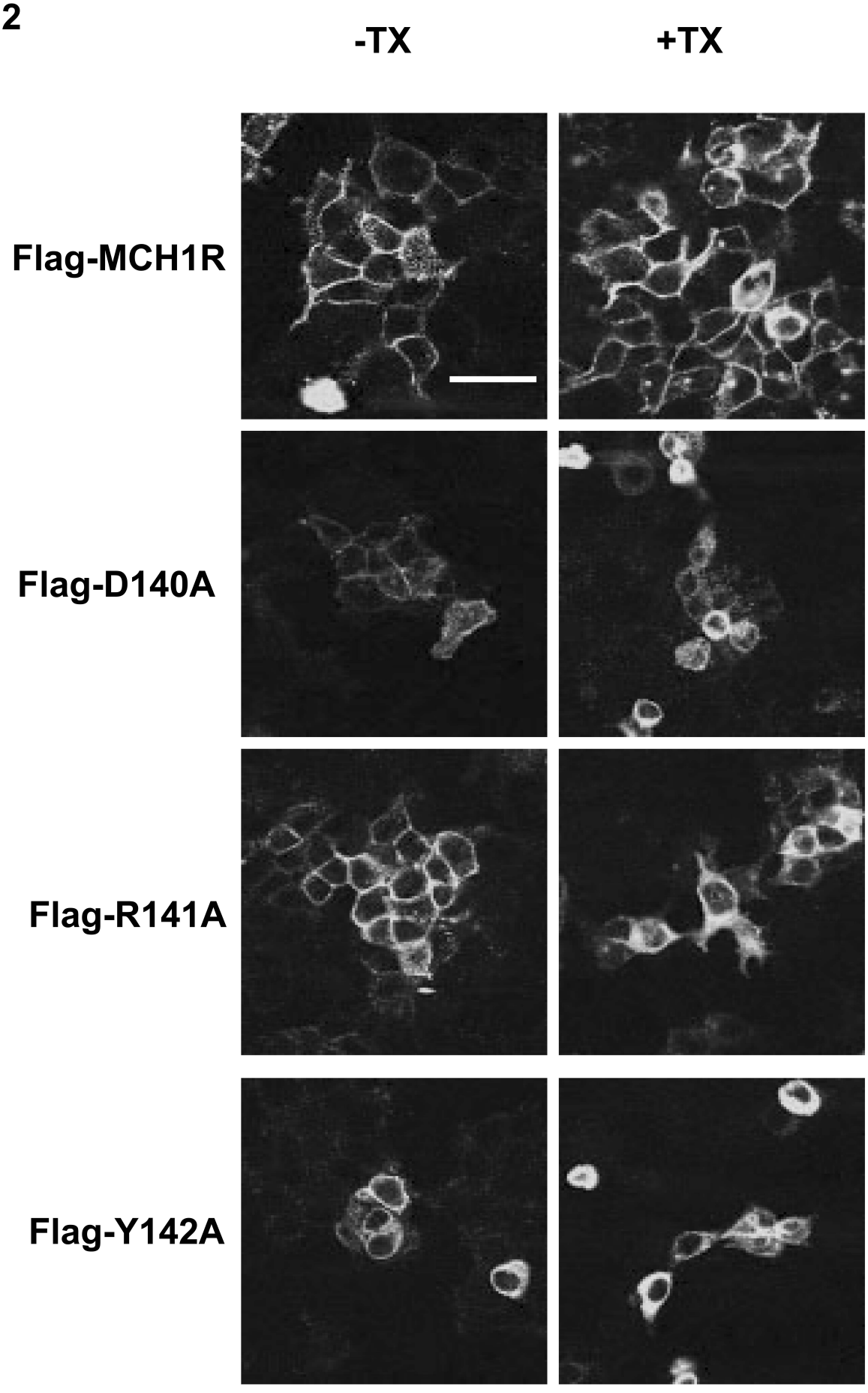

Fig.3

A

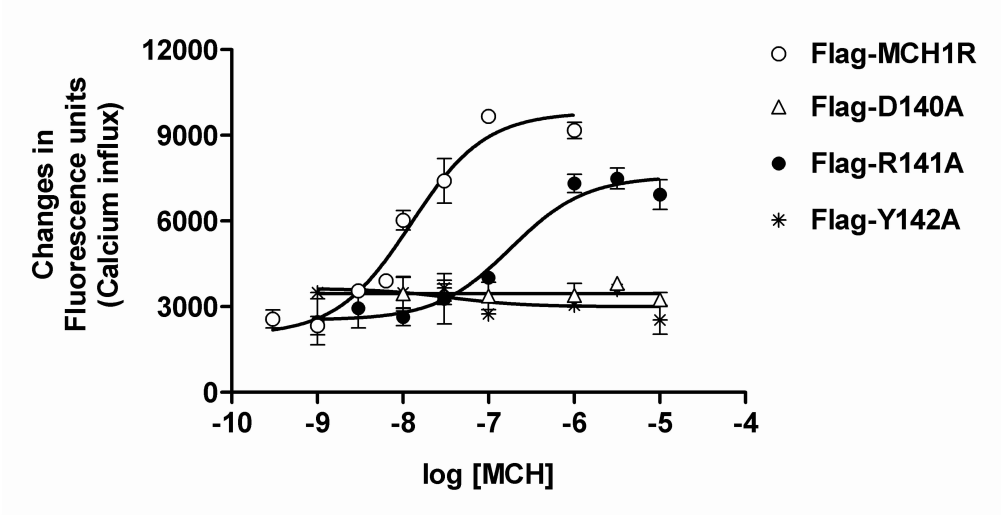
Changes in Fluorescence units (Calcium influx)
12000
9000
6000
3000
0
-10
-9
-8
-7
-6
-5
-4
log [MCH]
Flag-MCH1R
Flag-D140A
Flag-R141A
Flag-Y142A

B

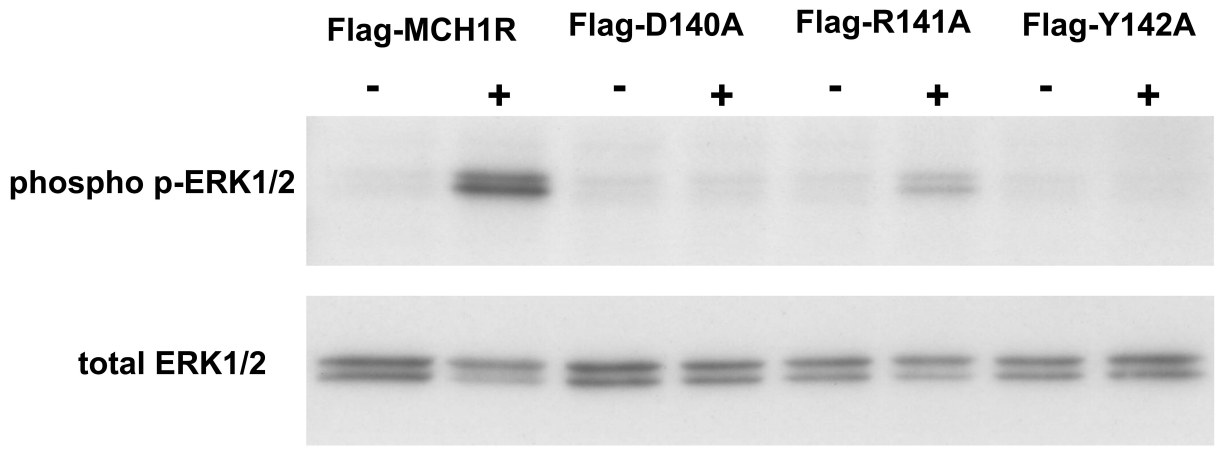
Flag-MCH1R
Flag-D140A
Flag-R141A
Flag-Y142A
-
+
-
+
-
+
-
+
phospho p-ERK1/2
total ERK1/2

C

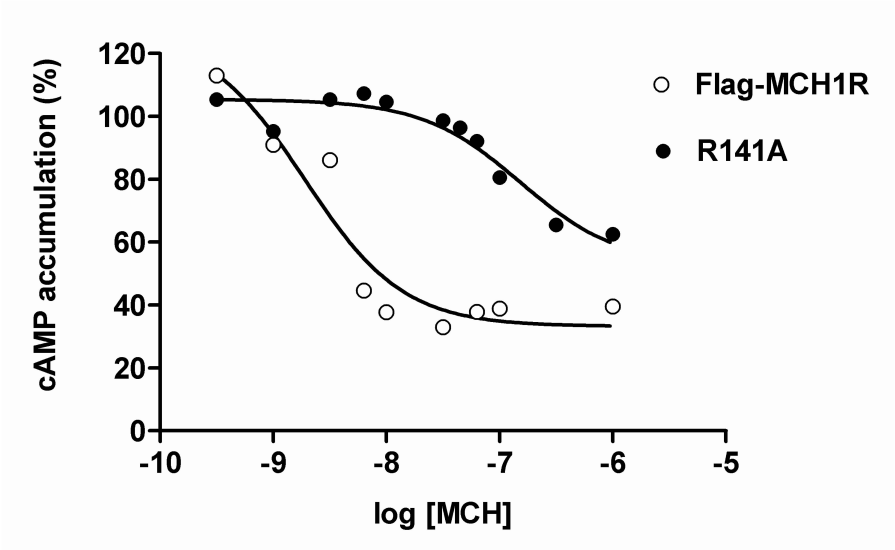
cAMP accumulation (%)
120
100
80
60
40
20
0
-10
-9
-8
-7
-6
-5
log [MCH]
Flag-MCH1R
R141A

Fig.4

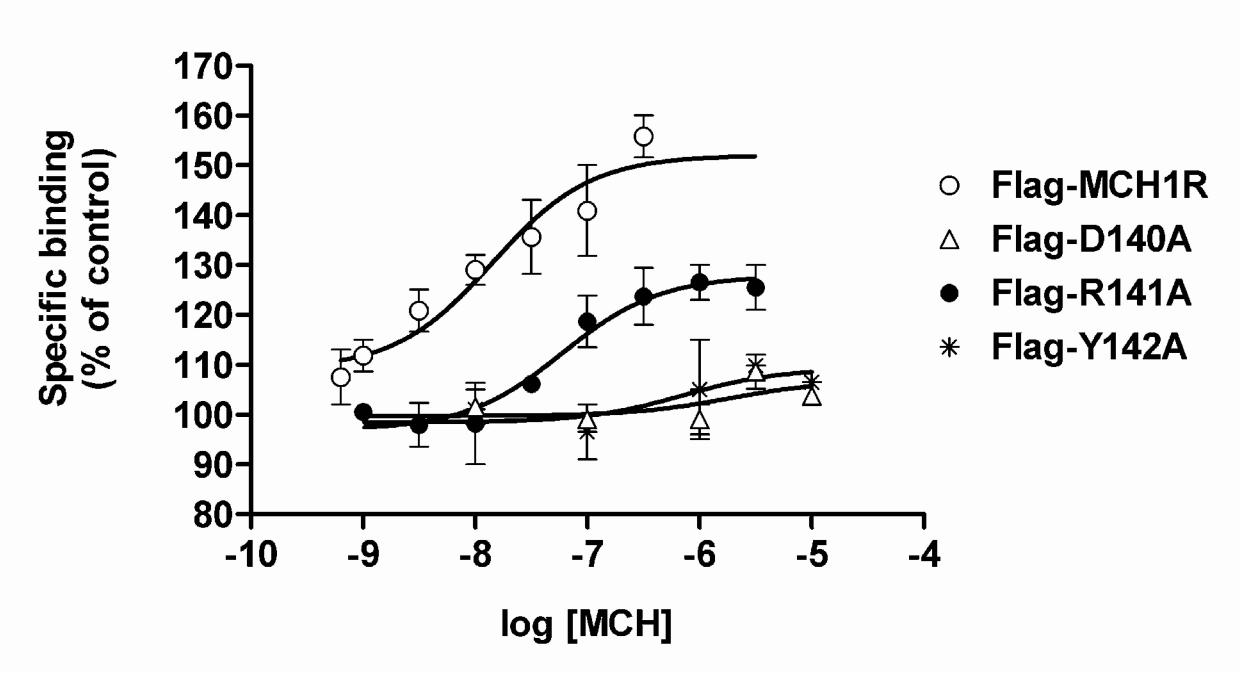
Specific binding
(% of control)
170
160
150
140
130
120
110
100
90
80
-10
-9
-8
-7
-6
-5
-4
log [MCH]
Flag-MCH1R
Flag-D140A
Flag-R141A
Flag-Y142A

TABLE 1

Specific radioligand binding of Flag-tagged MCH1R and the mutant receptors in transiently transfected HEK293T cells.

Receptor	K_d (nM)	B_{Max} (fmol/mg protein)
Flag-MCH1R	1.0 ± 0.1	217.5 ± 36.0
Flag-D140A	1.5 ± 0.3[a]	72.4 ± 12.9
Flag-R141A	3.8 ± 0.4[b]	156.0 ± 12.6
Flag-Y142A	1.8 ± 0.1[b]	82.7 ± 6.4

[a] $P < 0.05$, [b] $P < 0.01$, significantly different from Flag-MCH1R by Student's *t*-tests.

The results represent the mean ± SEM of three independent experiments.

TABLE 2

Signaling by Flag-tagged MCH1R and the mutant receptors after transfection into HEK293T cells.

Receptor	EC_{50} of MCH for calcium influx (nM)	Increase of ERK1/2 phosphorylation (basal as 100%, 1 μM MCH, 5 min)	EC_{50} of MCH on cAMP inhibition (nM)
Flag-MCH1R	6.8 ± 1.7	225.0 ± 35.6	1.5 ± 0.3
Flag-D140A	None	None	ND
Flag-R141A	246 ± 19.0	163.0 ± 23.0	148.3 ± 12.0
Flag-Y142A	None	None	ND

ND: not determined.

The data represent the mean±SEM of three independent experiments performed in duplicate.